Bulletin of Atmospheric Science and Technology (2020) 1:43–57
https://doi.org/10.1007/s42865-020-00004-7

RESEARCH ARTICLE

Multifractal Characteristics of Cloud-to-Ground Lightning Intensity Observed in AMMA-CATCH Station (Northern Benin)

M. Agbazo[1] · G. Koto N'Gobi[2] · A. J. Adéchinan[3] · B. Kounouhewa[2] · B. E. Houngninou[3] · A. Afouda[1]

Received: 7 May 2019 / Accepted: 31 January 2020 / Published online: 18 February 2020

Abstract
Cloud-to-Ground (CG) lightning intensity time series recorded in northern Benin, during days of monsoon season (summer 2006), has been deeply explored using multifractal framework. The results suggest the existence of strong multifractal characteristics in lightning intensity. However, detrending the data reduces the degree of multifractality. The multifractality arises from both a fat-tailed probability density function and long-range temporal correlations. But, the most dominant multifractality in lightning intensity series depends strongly on the kind of detrending that is retained from the profile during the multifractal detrended fluctuation analysis (MFDFA). These findings have allowed us to understand and characterize the complexity of lightning intensity structure in the network.

Keywords Lightning Intensity · Fractal Dimension · MFDFA · Multifractal · Benin

Introduction

Lightning is an atmospheric discharge phenomenon of nature occurring nearly fifty (50) times per second worldwide (Tapia et al. 1998). According to Telesca et al. (2008), the most accepted explanation for lightning is the friction and collision among ice and water particles, traveling in

✉ G. Koto N'Gobi
kotgabin36@yahoo.fr

1 International Chair in Physics Mathematics and Applications (CIPMA-Chair Unesco), Université d'Abomey-Calavi, BP : 526 UAC, Cotonou, Bénin

2 Laboratoire de Physique du Rayonnement (LPR), Université d'Abomey-Calavi, BP: 526 UAC, Cotonou, Bénin

3 Dépt. de Physique, Faculté des Sciences et Techniques, Université Nationale des Sciences, Technologies, Ingénierie et Mathématiques, Abomey, Bénin

convective drafts in the cloud. Moreover, thunderstorms are complex meteorological phenomena that involve several processes (dynamic, thermodynamic, microphysical, electrical, etc.). The electrical aspect of these phenomena results in natural, brief, and unpredictable discharges known as lightning (Tapia et al. 1998; Magi 2014).

Christian et al. (2003) have drawn a map of global electrical activities worldwide and note that the African continent's contribution into the global density of lightning is one of the most important in the world. According to these authors, the Congo Basin and a large part of West Africa, including Benin, are shown to be areas where electrical events are very remarkable during storms. Also, Betz et al. (2009b) have compiled in a single book of twenty-seven (27) chapters the results of many impressive researches related to lightning phenomena, gathered in some subtopics presented as follows: (a) the fundamental charging and discharge mechanisms of lightning; (b) the lightning detection networks in Europe, its observations from space and mapping channels; (c) the connection between lightning and higher atmosphere effects, including Schumann resonances around the globe; (d) the relation between lightning and microphysical parameters, precipitation, and strong storms; and (e) climate, chemistry, and important aspects about lightning protection (Betz et al. 2009b). Furthermore, Holler et al. (2009) reported lightning characteristics from four (4) continents, where sets of lightning measurements with emphasis on lightning NO_x production were done, during field campaigns. These campaigns were carried out in South Germany (Europe), Bauru area of Brazil (South America), Darwin area (North Australia), and Djougou area (West Benin). For West Africa, they concluded that the regional and temporal distributions of lightning vary accordingly to the fluctuations of few days and to long term seasonal variability, reflecting the West Africa monsoonal activity accompanied by the southward (northward) progression of the monsoon (Holler et al. 2009). The inter-continental comparisons of NO_x production within thunderstorms in Djougou area (Benin) show that standard strokes produce less NO_x by 40% in West Africa and Brazil than in North Australia and South Germany. Also, the negative intra-cloud lightning is said to contribute less in the production of NO than the total cloud-to-ground lightning in West Africa (Benin) comparatively to Australia, where the positive intra-cloud and cloud-to-ground lightning contribution is dominant (Holler et al. 2009).

Lightning is a disastrous weather phenomenon, particularly the cloud-to-ground ones which cause damages in many pieces of electric and electronic equipments, sensitive to electric and magnetic fields. For example, damages are noticed on wind power devices and photovoltaic systems (Martzloff 1989; Gill 2008). Lightning has damaged 3.9%, 8%, and 8.5% of turbines in Denmark, Germany, and Sweden, respectively. It also causes serious injuries leading to death in human and animals worldwide (Yuanlian and Yongfeng 2014). Study of Graham-Jones (2006) in the USA indicates that lightning can kill more than some of certain natural disasters. For instance, lightning killed 7741 people while 5268 death were related to tornadoes, 4481 to flood, and 1923 died through hurricanes from 1940 to 1981. Holle (2016) summarized the lightning-related death numbers per year in the world. They provide data for Africa (1417–1467), America (478), Asia (384), and Europe (24). So, high lightning-related death rate in Africa (poor continent) indicates that lightning-related death rates in less-developed countries are much higher than those in developed ones. The impacts are huge in other sectors such as health insurance, forestry, electricity (generation, transmission, and distribution), agriculture, telecommunication, transportation, and tourism (Mills et al. 2010). Unfortunately, there is no statistical data available to figure out the exact number of deaths and damages caused by lightning occurrence in Benin and other parts of West Africa.

For reducing the amount of physical and material damages caused by lightning, the understanding of its intrinsic characteristics as complex meteorological phenomenon is very important. But, natural phenomenon and climatic variables (e.g., lightning, solar radiation, precipitations, air temperature, wind speed, solar radiation, etc.) cannot be investigated using traditional statistical methods, such as discrete-time Fourier transform, linear correlation analysis, and power spectrum analysis (suitable for calculating relevant characteristics of stationary signals) because of their nonlinear, non-stationary, and complex nature (see, e.g., Zeng et al. 2013; Casdagli 1997; Ingle and Proakis 2000; Kantz and Schreiber 2004; Yang et al. 2016; Zhang et al. 2017a). Fractal methods are developed in literature and used to study the complex nature of lightning in several regions of the world (except in Africa, especially in Benin) to overcome the weakness of these traditional statistical methods (above mentioned). For example, in Brazil, the multifractal analysis of lightning channel for different categories of lightning has been done by Miranda and Sharma (2016). The results suggest that single lightning and multiple lightning have similar complexities in their channels. Telesca (2007) have studied the time-scaling analysis of lightning in Italy. They found the existence of time-clustering in the sequence of lightning time-occurrences, characterized by the presence of two scaling regions. Gou et al. (2007, 2009, 2010) have studied in China the complex nature of lightning. They found that the return stroke electric signals exhibit strong degree of multifractality and singularity. In Gou et al. (2009), it is observed that the fractal dimensions of the electric signals of radiation ranged from 1.2 to 1.5 with an average of 1.3.

During the African Monsoon Multidisciplinary Analysis (AMMA) project's campaign, AMMA-CATCH site in Benin has been one of the three strategic sites in West Africa (Benin, Niger, Mali) offering opportunity to study contrasted climatic areas (Redelsperger et al. 2006; Mamadou et al. 2014). For this, a lot of equipments have been installed in Northern Benin to measure several climatic and meteorological parameters (including lightning) for understanding climate strong variability in the region (Redelsperger et al. 2006). However, few efforts were dedicated to the framework of lightning studies. Some works have explored the relationships between lightning and other atmospheric parameters (related to lightning *NO* and *NOx* production), namely precipitations and thunderstorm's electrical activities in relation to the triggering parameters of these natural phenomena (Betz et al. 2009a; Holler et al. 2009; Houngninou et al. 2013; Adéchinan et al. 2014; Houngninou et al. 2017). Thus, the nonlinear characteristics of observed cloud-to-ground lightning intensities have not been studied yet. Also, as cloud-to-ground lightning is directly related to human being, it creates huge physical and material damages in several domains of existence. The finality of this study aims to reveal the complex behavior of cloud-to-ground lightning intensity reaching the soil, in the point of view of the probable damages that it can create to human. So, the objective of this study is to explore for the first time the multifractal characteristics of cloud-to-ground lightning intensity in Benin, as a beginning for understanding the complex characteristics of lightning. This step prepares future studies that will aim to quantify the cross-correlation between lightning and extreme precipitations by improved method (e.g., multifractal detrended cross-correlation analysis, MDCCA) instead of traditional cross-correlation analysis (TCA) methods (e.g., regression analysis, cluster analysis), based only on a single scale analysis and generally used in the study area (Houngninou et al. 2013, 2017; Adéchinan et al. 2014). The paper is organized as follows: in the "Materials and methods" section, the methods and the data set are described. Results and discussion are represented in the "Results and discussion" section. Finally, we conclude the paper with a summary and outlook for further research in the "Conclusions" section.

Materials and methods

Description of the measurement network

The study was carried out in AMMA-CATCH network in the northern part of Benin, characterized by a Sudanian climate. This region extends between latitudes 9° N to 10.4° N and longitudes 1.5° E to 3° N and covers an area of about 15,000 km^2, as indicated by the inner part of the border limiting the study area in Fig. 1a. There is one rainy season from March to October and a dry season the rest of the year. The total cumulative mean precipitation amount is ~ 1200 mm/year over the period 1954–2005. August is the rainiest month in the area (Lawin et al. 2010). The mean values of air temperature and relative humidity are respectively ~ 30 °C and ~ 80%. The area's relief is not marked; however, the country's highest relief point of ~ 658 m is located in the study area and known as "Atacora Mountains." Fig. 1b displays the topographical map of the study area, showing that Natitingou and Boukoumbe are in the highest relief level. The lightning measurement network is constituted by six sites: Natitingou, Bembereke, Boukoumbe, Djougou, Parakou, and Bassila, as shown in the Fig. 1. Around each site, intra-cloud lightning and cloud-to-ground strokes discrimination can be performed for 120-km radial distance.

Description of the materials

Lightning's location and their intensity are shown to be used for quantifying precipitations in numerous studies in addition to radar's reflectivity (Houngninou et al. 2013, 2017; Adéchinan et al. 2014). During the AMMA campaign, in-situ database of light-storm electrical activities was drawn from which data are used for the current study. A VLF/LF Lightning Network (LINET) equipped with several sensors was deployed, as one of the four (4) continents of

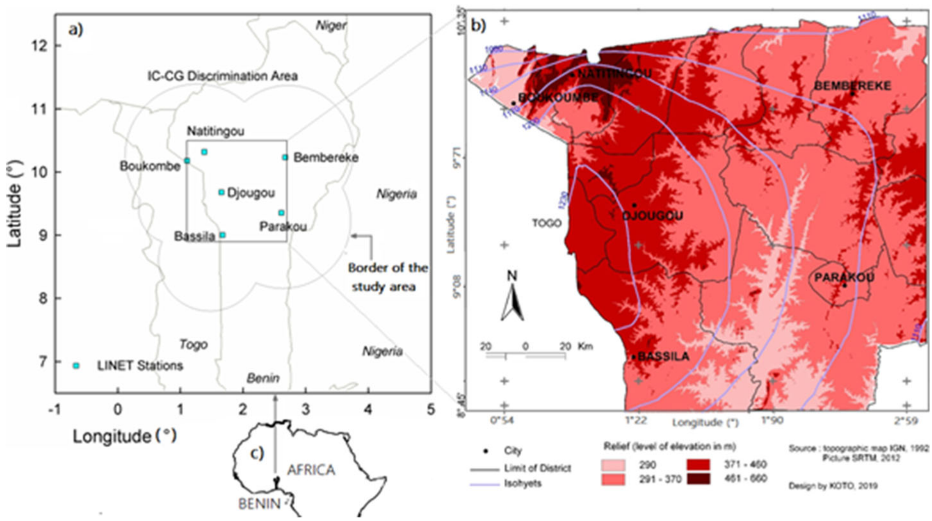

Fig. 1 LINET deployment in Benin during AMMA campaign (from June to November 2006) in Djougou area (West Africa). a) Map of Benin, showing the six stations of the LINET-Benin and the study area, modified from Holler et al. (2009). b) Hydro-topographical map of the study area, showing the level of elevation (m) in a Sudanian climate. c) Location of Benin in Africa

European international research network cooperation (Betz et al. 2008; Holler et al. 2009). LINET's functioning principle during AMMA is the same as described for European network in Betz et al. (2008) and Holler et al. (2009). Five modern features are specified in the network: (a) a total lightning capability, leading to the measurement of both cloud-to-ground strokes and intra-cloud (IC) lightning; (b) a low-amplitude reporting, capable of detecting discharge current below 5 kA within the central part of the network, whereby IC events dominate; (c) a 3D discrimination, utilizing a time-of-arrival (TOA) method to separate efficiently CG from IC and provided that the sensor baseline does not exceed ~250 km; (d) an IC emission height, permitting to determine the height of each cloud event; and (e) an optimization of the location accuracy leading ~150 m, an average value of strokes reaches positions (Betz et al. 2009a). LINET is a sensitive network working with 3D capability. Thus, intra-cloud lightning as well as cloud-to-ground flashes can be detected. The efficiency of the system allows for unprecedented low-amplitude detection power (Holler et al. 2009; Betz et al. 2009b). Since abundant IC events are located, an effective discrimination against CG is performed. Preferentially, the time-of-arrival method which required at least four stations recording data is used for locating the horizontal and vertical position of lightning strikes during measurement (Betz et al. 2004, 2008, 2009b). The system can measure the time and the horizontal and vertical location of VLF sources as well as the amplitude and the polarity of these events. In our study sites, each station of the LINET consists of (1) a crossed loop antenna for measuring the magnetic field, (2) a Global Positioning System (GPS) antenna for measuring the precise time reference, and (3) a personal computer (PC) for data acquisition and data storage. Figure 2 a presents the measurement equipment at Natitingou, a typical site of the AMMA-CATCH Lightning Network.

Description of the measurement process

The lightning detection principle is based on the measurement of the electromagnetic field in a frequency range VLF/LF. Indeed, each sensor of the system detects the electromagnetic pulse with a time delay proportional to the distance separating the antenna to the real location of the lightning. Since the speed of propagation of the wave and the distance between the sensors are constant, it is therefore sufficient to calculate the difference in arrival time existing between the sensors two by two and deduct a set of equations describing a hyperbolic shape. The intersection of these hyperboles is the unique solution that indicates the real location of the discharge. This technique known as *triangulation* requires at least three sensors with synchronized time base. Within or close (< 120 km) to the network, it is possible to discriminate cloud-to-ground lightning and intra-cloud lightning. Observations of more distant lightning are also possible for the stronger events. No lightning data is available in Benin before AMMA-CATCH campaign. Unfortunately, during this period in Benin, lightning data of only summer 2006 (June to November) has been recorded for experiments. A total number of 1,301,993 lightning events have been recorded. Despite the small size of the time series, the robustness of the method will not be affected because multifractal detrended fluctuation analysis (MFDFA, described below) is less sensitive to the size of the series (López and Contreras 2013). These data are of good quality so that several scientific research groups use them for a variety of purposes (see Holler et al. 2009). Both the high detection efficiency with the inclusion of IC events and the improved location accuracy represent interesting features that are exploited by numerous projects in atmospheric electricity (Holler et al. 2009; Betz et al. 2009a). In the current study, we use only cloud-to-ground data.

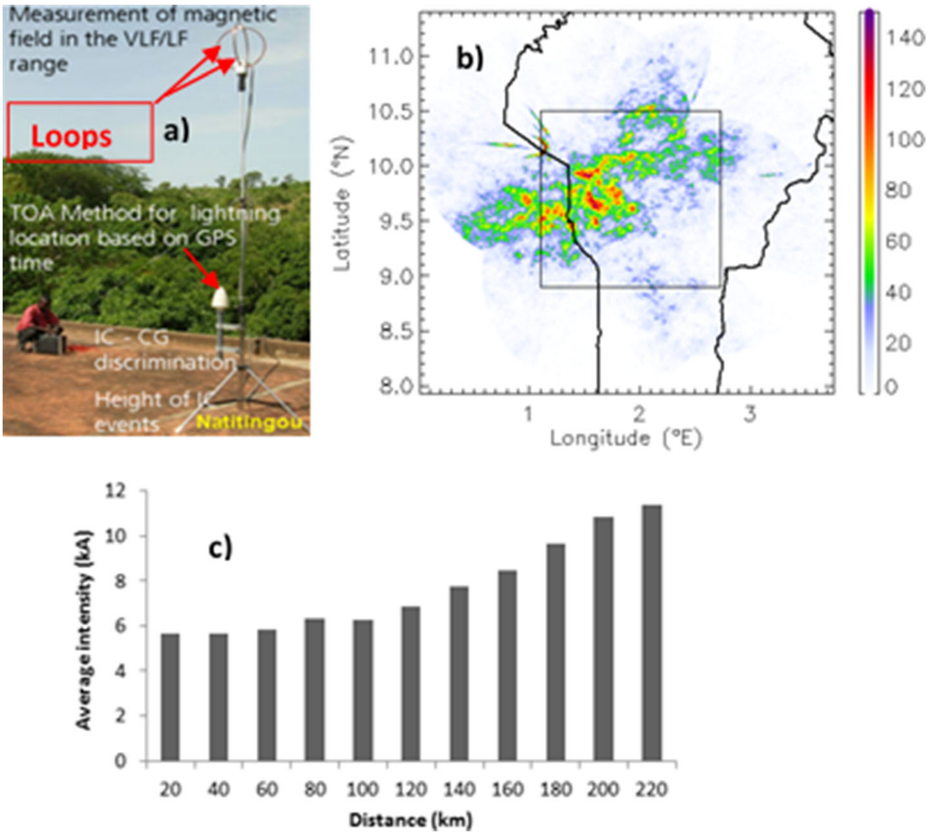

Fig. 2 a) LINET station installed in Natitingou (photo from the measurement fields). b) Seasonal cloud-to-ground lightning distribution in the study area. c) Effectiveness of the IC detection

Figure 2 b and c present respectively the seasonal cloud-to-ground lightning distribution and the effectiveness of the IC detection in the study area. One can notice that the mean intensity of cloud-to-ground lightning (Fig. 2c) increases when moving away from the center of the study area. The strongest variations are noticed after 120 km. So the analysis in this study should not be affected by the detection sensitivity to the distance.

Daily cloud-to-ground lightning intensities (negative and positive values) are used. Let us remember that no specific predefined time scale exists for studying lightning. So, we have used daily lightning average intensities comparatively to some other important meteorological parameters such as rain amount, air temperature, and solar power, in which variation can impact importantly human existence and which study required at least daily time scale. Let I_{CG} be the daily cloud-to-ground lightning intensity domain-averaged values. I_{CG} is calculated as follows:

$$I_{CG} = \frac{1}{N_i + N_j}\left(\sum_{n=1}^{N_i} |NI_{CG}(n)| + \sum_{m=1}^{N_j} PI_{CG}(m)\right) \quad (1)$$

where N_i and N_j are, respectively, the number of negative and positive cloud-to-ground lightning intensities observed during a chosen day in the period of measurement and NI_{CG} and PI_{CG} are respectively the negative and positive cloud-to-ground lightning intensities observed during a chosen day in the period of measurement.

The temporal variation of I_{CG} time series and the daily number of lightning events are presented in Fig. 3. We notice a strong variation of both daily cloud-to-ground lightning intensities and lightning numbers during the study period.

Box counting method

The fractal dimension is computed by using the box counting method (Mandelbrot 1982; Lovejoy et al. 1987; Hubert and Carbonnel 1989). Let T be the total observation time; it is divided into n contiguous intervals of length λ taken as successive powers of 2 $\{2^0, 2^1, 2^2\ldots\}$. The total number of occupied intervals, $N(\lambda)$, in which at least one lightning intensity greater than or equal to a given threshold, Th, is counted. If the data forms a one-dimension fractal, then

$$N(\lambda) \propto \lambda^{-D_f} \tag{2}$$

$$\log(N(\lambda)) = -D_f \log(\lambda) + K \tag{3}$$

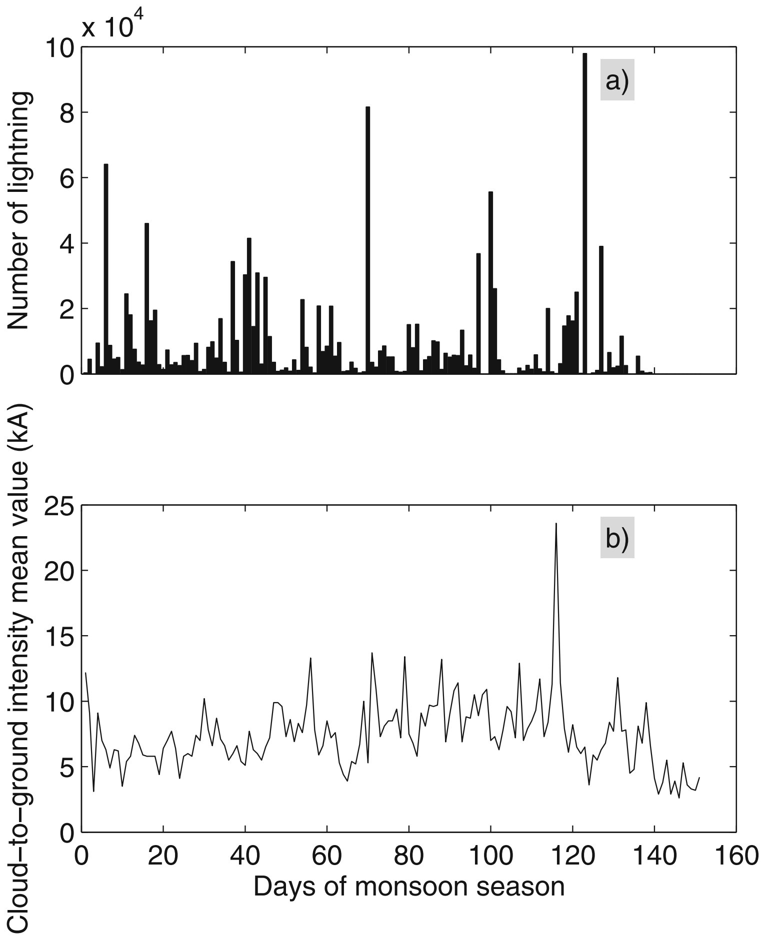

Fig. 3 Variation of lightning time series during the days of monsoon season in 2006. a) Daily cloud-to-ground lightning numbers. b) Daily cloud-to-ground lightning intensities

where K is constant and D_f is defined as the fractal dimension. When plotting $log(N(\lambda))$ as a function of $log(\lambda)$, a straight line with slope $(-D_f)$ is obtained. In this study, the fractal dimension of each lightning intensity data is performed at various thresholds (Th), namely $\{0, 0.5, 1 \text{ and } 1.5\}M$, where M is the mean value of lightning intensity data.

According to Lee et al. (2006), the critical temporal scale (Cts) is defined as the value of λ at the intersection of straight lines with $D_f < 1$ and that with $D_f = 1$, for each threshold. The lightning intensity exceeding the threshold Th could occur when time scale is greater than or equal to the critical scale.

Multifractal detrended fluctuation analysis

To investigate multifractal characteristics of non-stationary, nonlinear, natural, and complex meteorological phenomenon time series (Shen et al. 2017; Wan et al. 2016; Jiang et al. 2017), the MFDFA method was proposed by Kantelhardt et al. (2002). It can be briefly described as follows (Shen et al. 2017):

Let $\{x_t| t = 1, 2, \ldots, N\}$ be an original time series of N equidistant measurements to which the procedure of the MFDFA method is applied. First, a new series named "profile" is determined as follows:

$$Y(k) = \sum_{t=1}^{k} (x_t - < x >) \tag{4}$$

where $<x>$ is the mean value of x_t and $k = 1, 2, \ldots, N$.

The profile is then divided into $N = int(N/s)$ equal-sized nonoverlapping windows with a length s. Since N is not the integral multiple of s in most of the cases, there might be a short part at the end of the profile that remains uncovered. To take full account of the series, the same procedure can be repeated starting from the end of the series. Hence, we obtain $2Ns$ segments altogether. We then calculate the variance of each window as

$$F^2(\nu,s) = \begin{cases} \frac{1}{s}\sum_{i=1}^{s}\left\{Y_{[(\nu-1)s+i]} - y_\nu^{(m)}(\mathrm{i})\right\}^2 \text{ for } \nu = 1,2,\ldots,N_s \\ \frac{1}{s}\sum_{i=1}^{s}\left\{Y_{[N-(\nu-N_s)s+i]} - y_\nu^{(m)}(\mathrm{i})\right\}^2 \text{ for } \nu = (N_s+1),..,2N_s \end{cases} \tag{5}$$

It should be noted that linear (i.e., polynomial order $m = 1$), quadratic (i.e., $m = 2$), cubic (i.e., $m = 3$), or higher order polynomials $y_\nu^{(m)}(\mathrm{i})$ can be used to fit the local trend, and MFDFA is noted as MFDFA1, MFDFA2, MFDFA3, MFDFA4, etc. Multifractal fluctuation analysis (MFFA) corresponds to a case in which any kind of detrending is retained from the profile. In MFDFAm, possible m order trends are eliminated in the profile. By averaging over all windows, we obtain the fluctuation as

$$F_q(s) = \begin{cases} \left\{\frac{1}{2N_s}\sum_{\nu=1}^{2N_s}\left[F^2(\nu,s)\right]^{q/2}\right\}^{1/q} \text{ for } q \neq 0 \\ exp\left\{\frac{1}{4N_s}\sum_{\nu=1}^{2N_s}\ln\left[F^2(\nu,s)\right]\right\} \text{ for } q = 0 \end{cases} \tag{6}$$

where q is the order of moment. If the time series follow the power law, then we can obtain the scaling function

$$F_q(s) \propto s^{h(q)} \tag{7}$$

where $h(q)$ is the generalized Hurst scaling function (Kantelhardt et al. 2002; Telesca et al. 2004). For monofractal time series, $h(q)$ is independent of q, whereas, for a multifractal time series, $h(q)$ varies with q. This dependence is considered to be a characteristic of multifractal process (Kantelhardt et al. 2002). In order to avoid a divergence of moments in the fat tails of the fluctuation distribution as mentioned by some authors (Wang et al. 2013; Ihlen 2012), we restrict the order q within the range $-5 \leq q \leq 5$ as in Wang et al. (2013).

Multifractal spectrum

In order to get more information about the lightning intensity data and to characterize the strength of the multifractality, two functions and parameters are deduced from $h(q)$ via the Legendre transform (Feder 1988; Kantelhardt et al. 2002; Shi et al. 2008; Liu et al. 2014a, b; Jiang et al. 2016). These functions are defined by following equations:

$$\begin{cases} \alpha(q) = h(q) + q\dfrac{dh(q)}{dq} \\ f(\alpha) = q[\alpha - h(q)] + 1 \end{cases} \tag{8}$$

$\alpha(q)$ and $f(\alpha)$ are respectively singularity exponent and multi-scales fractal spectrum.

These parameters are defined as follows:

$$\Delta\alpha = \alpha_{\max} - \alpha_{\min} \tag{9}$$

and

$$\Delta f = f(\alpha_{\min}) - f(\alpha_{\max}) \tag{10}$$

where $\alpha_{\max}$ and $\alpha_{\min}$ are obtained from the relation $f(\alpha) = 0$.

If the observed time series is a single-scale fractal series, the function $f(\alpha)$ is constant. Generally, if the time series is a multi-scale series, the function $f(\alpha)$ has a bell-like shape. The parameter $\Delta\alpha$ describes the inhomogeneity of the distribution of probability measured on the overall fractal structure, which has been identified as the intermittency and degree of multifractality (Liu et al. 2014a, b). $\Delta\alpha$ is multifractal spectrum width. The smaller $\Delta\alpha$ indicates that the fractal region is more uniformly distributed, while the bigger $\Delta\alpha$ implies that the probability distribution is more heterogeneous. $\Delta f > 0$ shows that the number of the largest subsets is greater than the minimal one in probability measures, so, multi-scale fractal spectrum shows a “left hook” shape; $\Delta f < 0$ shows the contrast condition, and the multi-scale fractal spectrum is “right hook” shape.

Origins of multifractality

Generally, there are two major types of sources for multifractality in time series: (a) different temporal correlations for small and large fluctuations and (b) a fat-tailed probability distribution for the values of the time series (Rak and Zieba 2015). The main methods to find the contributions of the two sources of multifractality are the shuffling procedure and the surrogating procedure, respectively (Kwapien et al. 2005). Indeed, to test the first source of multifractality, we randomly shuffle the series to remove any temporal correlations. Thus, if no multifractal feature remains after we conduct the shuffling procedure on the original multifractal series, we can conclude that long-range correlation dominates the multifractality in the original series. The shuffling procedure consists of generating a random permutation of the array elements of time series. In contrast, surrogate data is used to check whether the multifractality comes from fat-tailed probability distribution, because it can eliminate any sort of nonlinearities in original series and weaken the non-Gaussianity of the distributions. In this paper, we use the common method of amplitude adjusted Fourier transform (AAFT) developed in Theiler et al. (1992), Dong et al. (2017), and Wu et al. (2018) to obtain surrogate data. AAFT can be summarized according to Dong et al. (2017) as follows: (1) a discrete Fourier transform of the original series is conducted, (2) the discrete Fourier transform of the data is multiplied by random phases, and (3) an inverse Fourier transform is performed to generate a phase randomized surrogate. To further compare the contributions of multifractality from the two sources, the corresponding multifractal spectrum width is computed for the original series, shuffled series, and surrogated series.

Results and discussion

Figure 4 presents the results of applying the box counting method, with different thresholds (*Th*). Box counting results are practically the same for *Th* {0; 0.5}*M*. However, it is observed that the critical temporal scale is an increasing function of *Th*. This result implies the existence of multifractal characteristics in lightning intensity.

Figure 5 a–c present respectively the variation of the generalized $h(q)$, the singularity spectrum function $f(\alpha)$, and the singularity exponent function $\alpha(q)$ obtained using MFFA and MFDFA1–4. It is important to remember that in MFFA, any kind of detrending is retained in the profile. Figure 5 a shows the generalized Hurst exponents $h(q)$ with varying moments

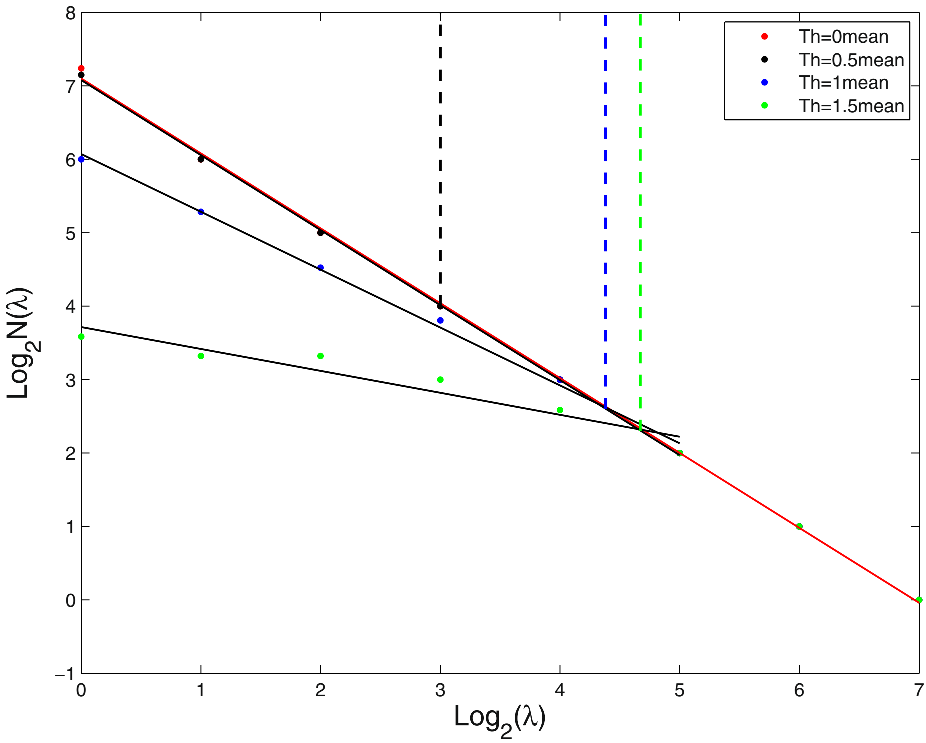

Fig. 4 $log(N(\lambda))$ versus $log(\lambda)$ for different thresholds (*Th*): the abscises values on the horizontal axis of the intersection points between the straight lines (in black color), corresponding to each threshold curve and the vertical dash lines (in black, blue, and green color) respectively, indicate the critical temporal scale (*Cts*)

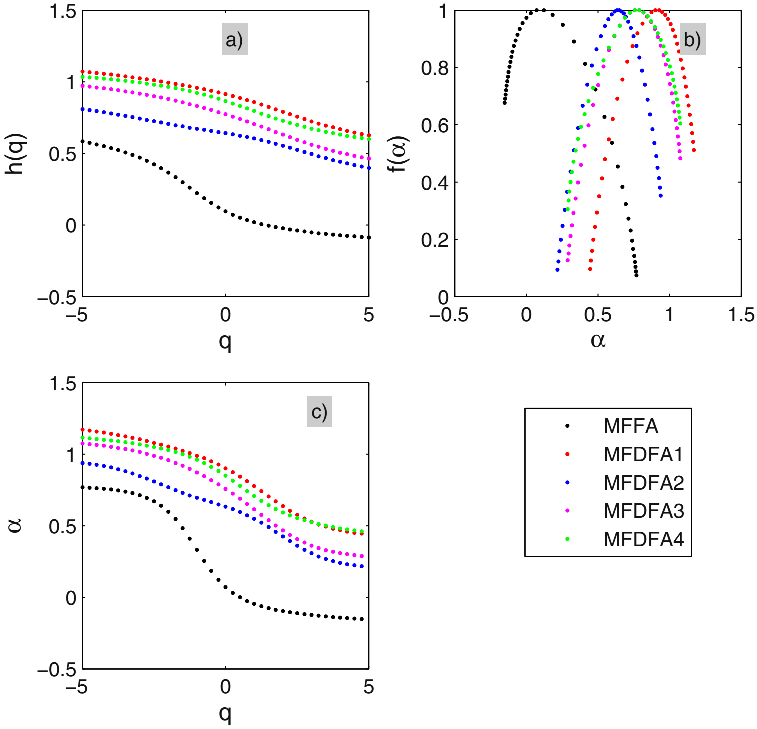

Fig. 5 a) Generalized Hurst exponent $h(q)$, b) singularity spectrum $f(\alpha)$, and c) singularity exponent $\alpha(q)$ obtained using MFFA and MFDFA1–4

($q = 5, 4, 3, 2, 1, -1, -2, -3, -4, -5$). It is observed that whatever the method used (MFFA or MFDFA1–4), the exponents $h(q)$ decreases with the increase values of the moment q which indicate the presence of the strong multifractal behavior in lightning intensity series. However, the exponents $h(q)$ change little with the increasing values of q when m ($m = 1, 2, 3, 4$) order trends are eliminated in the profile, indicating the weak multifractal behavior.

The multifractal spectrum $f(\alpha)$ obtained by MFFA and MFDFA1–4 versus α are shown in Fig. 5b. The curves have a bell-like shape and confirm the strong multifractal characteristics of the lightning intensity series. Figure 5 c presents the relationship between $\alpha(q)$ and the moment q. Their shapes also confirm the strong multifractal characteristics. To measure the strength of this multifractality, the multifractal spectrum analysis has been done.

Figure 6 presents the variation of $\Delta\alpha$, and Δf versus the degree m of the local polynomial trend when MFFA and MFDFA1–4 methods are used. MFFA is represented by $m = 0$. It is observed that $\Delta\alpha$ is positive whatever the used values of m. Generally, $\Delta\alpha$ values obtained with MFFA is greater than those obtained when m ($m = 1, 2, 3, 4$) order trends are eliminated (MFDFA1–4). Therefore, lightning intensity presents a stochastic dynamic character and strong fluctuations (Zeng et al. 2013). The maximum $\Delta\alpha$ shows strongest multifractal characteristics. So, detrending the data reduces the degree of multifractality. However, when the fourth-order trends are eliminated (MFDFA4), the smaller $\Delta\alpha$ is obtained, indicating that the fractal region is more uniformly distributed. It is observed that $\Delta f > 0$, when MFFA is applied. This result shows that the number of the largest subsets is greater than the minimal one in

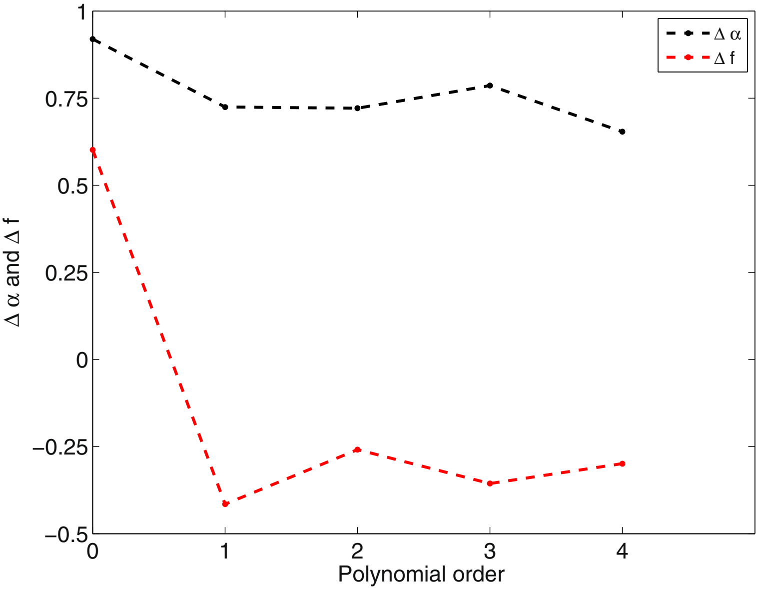

Fig. 6 $\Delta\alpha$- and Δf-m plots of lightning intensity series obtained using MFFA (when m = 0) and MFDFA1–4 (m = 1, 2, 3, 4)

probability measures. The contrasted results are obtained when MFDFA1–4 is applied. The fractal properties of the series change accordingly to the kind of trend.

The multifractal spectrum width and the $\Delta\alpha$ of original, shuffled, and surrogated series are shown in Fig. 7. It is found that when any kind of trend is retained in the profile (i.e., MFFA is

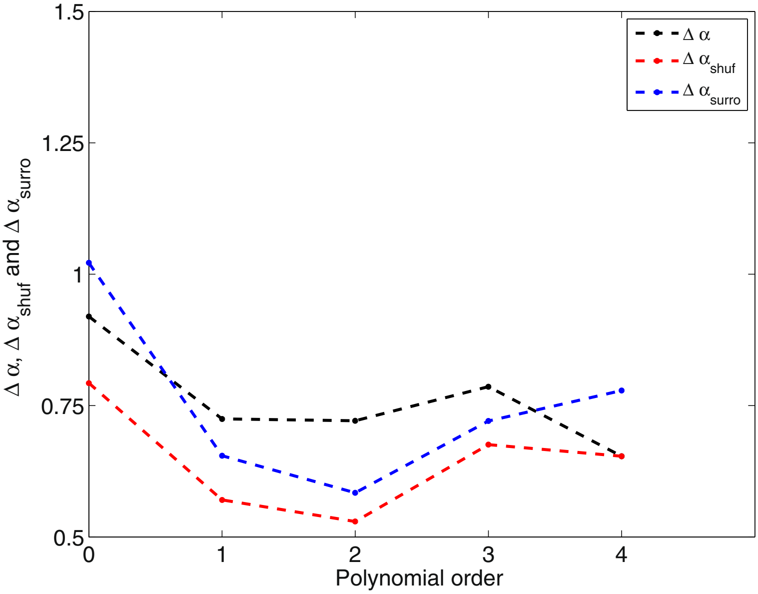

Fig. 7 $\Delta\alpha$-m plots of lightning intensity series obtained using MFFA (when m = 0) and MFDFA1–4 (m = 1, 2, 3, 4) for original, shuffled, and surrogated data

applied) or when the fourth-order trends are eliminated (MFDFA4), $\Delta\alpha_{shuf} < \Delta\alpha_{surro}$; thus, the multifractality due to fat-tailed probability is the most dominant multifractality in lightning intensity series. However, when m ($m = 1, 2, 3, 4$) order trends are eliminated (MFDFA1–4), the range of change of $\Delta\alpha$ is significantly reduced after the original series is shuffled and surrogated, indicating a reduction in the degree of multifractality. Moreover, $\Delta\alpha_{\mathrm{surro}} < \Delta\alpha_{\mathrm{shuf}} < \Delta\alpha$, so, in these cases, the strength of the long-range correlation multifractality is greater than that of the fat-tailed probability distribution multifractality. Therefore, the multifractality arises from both a fat-tailed probability density function and long-range temporal correlations. From these results, one can note that the multifractal characteristics, the multifractality degree and the origin of multifractality depend strongly on the kind of detrending that is retained.

Conclusions

The analysis performed in this study aims to explore for the first time the multifractal characteristics of lightning intensity in Benin. Daily cloud-to-ground lightning intensities (negative and positive values) measured in northern Benin during days of monsoon season for 2006 are cumulated to draw a set of daily lightning intensity time series. Box counting method is applied to obtain the critical temporal scale (*Cts*) for different thresholds. The multifractal detrended fluctuation analysis (MFDFA) is used to investigate the multifractal properties.

The results of applying box counting method with different thresholds (*Th*) show that *Cts* is an increasing function of *Th*. Therefore, multifractal characteristics exist in lightning intensity. The results related to the application of MFDFA method reveal the presence of the strong multifractal behavior in lightning intensity series. However, the multifractal characteristics, the multifractality degree, and the origin of multifractality depend strongly on the kind of detrending which is applied to the data in the MFDFA method. Generally, the detrended reduces the degree of multifractality. The multifractality arises from both a fat-tailed probability density function and long-range temporal correlations. But, the most dominant multifractality in lightning intensity series depends strongly on the kind of trend eliminated in MFDFA method. These findings are important in understanding the complexity of lightning intensity structure in the network. Then, traditional cross-correlation analysis (TCA) methods are inappropriate and can provide erroneous or spurious results in cross-correlation of lightning intensity with other parameters (e.g., extreme precipitations). They are not in a position to fully characterize processes driven by nonlinear and multifractal characteristics with high degree of temporal variability as for lightning time series. Therefore, to overcome this problem, our future studies will aim to quantify the cross-correlation between lightning and extreme precipitations by multifractal detrended cross-correlation analysis (MDCCA).

Acknowledgments The authors would like to thank the African Monsoon Multidisciplinary Analysis (AMMA) project campaign for providing lightning data. We also express their great appreciation to the editor and the anonymous referees for their valuable suggestions.

Compliance with ethical standards

Conflict of interest The authors declare that they have no conflict of interest.

References

Adéchinan AJ, Houngninou EB, Kougbéagbédé H (2014) Relationships between lightning and rainfall intensities during rainy events in Benin. Int J Innov Sci Res 9(2):765–776

Betz HD, Schmidt K, Oettinger WP, Wirz M (2004) Lightning detection with 3D-discrimination of intra cloud and cloud-to-ground discharges. J Geophys Res Lett 31:L11108. https://doi.org/10.1029/2004GL019821

Betz, HD, Schmidt K, Oettinger WP, Montag B (2008) Cell-tracking with lightning data from LINET. Adv Geosci, 17:55–61, 2008. www.adv-geosci.net/17/55/2008/

Betz HD, Schmidt K, Laroche P, Blanchet P, Oettinger WP, Defer E, Dziewit Z, Konarski J (2009a) LINET-an international lightning detection network in Europe. Atmos Res 91:564–573

Betz HD, Schumann U, Laroche P (ed.) (2009b) Lightning: principles, instruments and applications. Review of Modern Lightning Research, eBook, Springer

Casdagli MC (1997) Recurrence plots revisited. Physica D: Nonlinear Phenomena 108 (1–2):12–44

Christian HJ, Blakeslee RJ, Boccippio DJ, Boeck WL, Buechler DE, Driscoll KT, Stewart MF (2003) Global frequency and distribution of lightning as observed from space by the optical transient detector. J Geophys Res 108:4005–4015

Dong Q, Wang Y, Li P (2017) Multifractal behavior of an air pollutant time series and the relevance to the predictability. Environ Pollut 222:444–457

Feder J (1988) Fractals. Plenum Press, New York

Gill T (2008) A lightning climatology of South Africa for the first two years of operation of the South African weather service lightning detection network: 2006–2007

Gou X, Zhang Y, Dong W, Qie X (2007) Wavelet-based multifractal analysis of the radiation field of first return stroke in cloud-to-ground discharge. Chin J Geophys 50(1):104–109

Gou X, Chen M, Zhang Y, Dong W, Qie X (2009) Wavelet multiresolution based multifractal analysis of electric fields by lightning return strokes. Atmos Res 91:410–415

Gou X, Chen M, Du Y, Dong W (2010) Fractal dynamics analysis of the VHF radiation pulses during initial breakdown process of lightning. Geophys Res Lett 37:L11808. https://doi.org/10.1029/2010GL043178

Graham-Jones BC (2006) The fractal nature of lightning: an investigation of the fractal relationship of the structure of lightning to terrain. Treatises and Dissertations, The Florida State University, pp: 122. http://fsu.digital.flvc.org/

Holle RL (2016) Lightning-caused deaths and injuires related to agriculture, paper presented at Intl. Conf. Lightning Meteorology, Vaisala, San Diego, Cal., 4 pp.

Holler H, Betz HD, Schmidt K, Calheiros RV, May P, Houngninou E, Scialom G (2009) Lightning characteristics observed by a VLF/LF lightning detection network (LINET) in Brazil, Australia, Africa and Germany. Atmos Chem Phys 9:7795–7824 www.atmos-chem-phys.net/9/7795/2009/

Houngninou EB, Adéchinan AJ, Moumouni S, Guédjé CF, Allé UC, Houngninou E, Kougbéagbédé H (2013) Relation entre éclairs nuage-sol et précipitations pendant la mousson de 2006 au Bénin. Eur J Sci Res 115(1):122–132

Houngninou EB, Adéchinan AJ, Guédjé KF, Onah MW, Kougbéagbédé H (2017) Relationships between lightning and insolation during monsoon season in Benin. Res J Phys Sci 5(9):1–5

Hubert P, Carbonnel JP (1989) Dimensions fractales de l'occurrence de pluie en climat soudano-sahélien. Hydrol Cont 4(1):3–10

Ihlen EA (2012) Introduction to multifractal detrended fluctuation analysis in matlab. Front Physiol 3:141–159

Ingle VK, Proakis JG (2000) Digital signal processing using MATLAB. Brooks/Cole Publishing Company, Pacific Grove

Jiang L, Zhang J, Liu X, Li F (2016) Multi-fractal scaling comparison of the air temperature and the surface temperature over China. Physica A 462:783–792

Jiang L, Zhao L, Zhao Z (2017) On the difference of scaling properties for temperature and precipitation over China. Adv in Meteo, vol. 2017, Article ID 5761275

Kantelhardt JW, Zschiegner SA, Koscielny-Bunde E, Havlin S, Bunde A, Stanley HE (2002) Multifractal detrended fluctuation analysis of nonstationary time series. Physica A: Statistical Mechanics and Its Applications 316:87–114

Kantz H, Schreiber T (2004) Nonlinear time series analysis, 2nd edn. Cambridge University Press, Cambridge

Kwapien J, Oswiecimka P, Drozdz S (2005) Components of multifractality in high frequency stock returns. Phys A Stat Mech its Appl 350:466e474

Lawin EA, Afouda A, Gosset M, Lebel T (2010) Caractéristiques évènementielles des pluies en zone soudanienne : apport des données à haute résolution amma catch à l'analyse de la variabilité de la mousson ouest africaine en climat soudanien. Annales des sciences Agronomiques du Bénin 13(1):1–22

Lee CK, Juang LC, Wang CC, Liao YY, Yu CC, Liu YC, Ho DS (2006) Scaling characteristics in ozone concentration time series (OCTS). Chemosphere 62(6):934–946

Liu ZH, Xu JH, Chen ZS, Ni Q, Wei CM (2014a) Multifractal and long-term memory of humidity processing the Tarim River basin. Stoch Environ Res Risk Assess 28:1383–1400
Liu Z, Xu J, Shi K (2014b) Self-organized criticality of climate change. Hin adv in meteo:685–691
López JL, Contreras JG (2013) Performance of multifractal detrended fluctuation analysis on short time series. Phys Rev E 87:022918
Lovejoy S, Schertzer D, Tsoni AA (1987) Functional box-counting and multiple elliptical dimensions of rain. Science 80:1036–1038
Magi B (2014) Global lightning parameterization from CMIP5 climate model output. J Atmos Oceanic Technol 32:434–452
Mamadou O, Cohard JM, Galle S, Awanou CN, Diedhiou A, Kounouhewa B, Peugeot C (2014) Energy fluxes and surface characteristics over a cultivated area in Benin: daily and seasonal dynamics 893–914
Mandelbrot BB (1982) The fractal geometry of nature. W.H. Freeman and Co., New York
Martzloff FD (1989) Lightning and surge protection of photovoltaic installations two case histories: Vulcano and Kythnos. Partial reprint of NISTIR-89 –4113
Mills B, Unrau D, Pentelow L, Spring K (2010) Assessment of lightning-related damages and disruption in Canada. Nat Hazards 52:481–499
Miranda FJ, Sharma SR (2016) Multifractal analysis of lightning channel for different categories of lightning. J Atmos and Solar-Terr Phys 45:34–44
Rak R, Zieba P (2015) Multifractal flexibly detrended fluctuation analysis. Acta Phys Pol B 46:1925
Redelsperger JL, Thorncroft CD, Diedhiou A, Lebel T, Parker DJ, Polcher J (2006) African monsoon multidisciplinary analysis: an international research project and field campaign. B Am Meteorol Soc 87:1739–1746. https://doi.org/10.1175/BAMS-87-12-1739
Shen Z, Shi J, Lei Y (2017) Comparison of the long-range climate memory in outgoing longwave radiation over the Tibetan Plateau and the Indian Monsoon Region. Adv in Meteo, vol. 2017, Article ID 7637351
Shi K, Liu CQ, Ai NS, Zhang XH (2008) Using three methods to investigate time–scaling properties in air pollution indexes time series. Nonlinear Anal Appl 9:693–707
Tapia A, Smith JA, Dixon M (1998) Estimation of convective rainfall from lightning observations. J Appl Meteorol 37:1497–1509
Telesca L (2007) Time-clustering of natural hazards. Nat Hazards 40(3):593–601
Telesca L, Balasco M, Colangelo G, Lapenna V, Macchiato M (2004) Investigating the multifractal properties of geoelectrical signals measured in southern Italy. Physics and Chemistry of the Earth, Parts A/B/C 29(295–303):2004
Telesca L, Bernardi M, Rovelli C (2008) Time-scaling analysis of lightning in Italy. Communications in Nonlinear Science and Numerical Simulation, 13:1384–1396. ScienceDirect: www.elsevier.com/locate/cnsns
Theiler J, Eubank S, Longtin A, Galdrikian B, Farmer JD (1992) Testing for nonlinearity in time series: the method of surrogate data. Physica D 58:77–94
Wan S, Liu Q, Zou J, He W (2016) Nonlinearity and fractal properties of climate change during the past 500 years in northwestern China. Discrete Dynamics in Nature and Society, vol. 2016, Article ID 4269431
Wang J, Shang P, Dong K (2013) Effect of linear and nonlinear filters on multifractal analysis. Appl Math Comput 224:337–345
Wu L, Chen L, Ding Y, Zhao T (2018) Testing for the source of multifractality in water level records. Physica A 508:824–839
Yang P, Wang G, Zhang F, Zhou X (2016) Causality of global warming seen from observations: a scale analysis of driving force of the surface air temperature time series in the Northern Hemisphere. Climate Dynamics 46 (9-10):3197–3204
Yuanlian H, Yongfeng Q (2014) Enhancement of lightning electric field signals using empirical mode decomposition method. IEEE, 978-1-4799-6284-6/14
Zeng Z, Yang H, Zhao R, Meng J (2013) Nonlinear characteristics of observed solar radiation data. Sol Energy 87:204–218
Zhang F, Yang P, Fraedrich K, Zhou X, Wang G, Li J (2017a) Reconstruction of driving forces from nonstationary time series including stationary regions and application to climate change. Physica A: Statistical Mechanics and its Applications 473:337–343